Mansoura Engineering Journal

Volume 17 | Issue 4 Article 6

12-1-2021

Analysis of Single Phase Induction Motor Performance Characteristics.

Ibrahim Amin
Electrical Engineering Department., Faculty of Engineering., Suez Canal University., Port-Said., Egypt.

Hassan El-Deeb
Electrical Engineering Department., Faculty of Engineering., Suez Canal University., Port-Said., Egypt.

Arafa Helal
Electrical Engineering Department., Faculty of Engineering., Suez Canal University., Port-Said., Egypt.

Recommended Citation

Amin, Ibrahim; El-Deeb, Hassan; and Helal, Arafa (2021) "Analysis of Single Phase Induction Motor Performance Characteristics.," *Mansoura Engineering Journal*: Vol. 17 : Iss. 4 , Article 6.
Available at: https://doi.org/10.21608/bfemu.2021.188700

ANALYSIS OF SINGLE PHASE INDUCTION MOTOR PERFORMANCE CHARACTERISTICS

Ibrahim A. Amin Hassan E. El-Deeb Arafa A. Helal
Electrical Engineering Dept., Faculty of Eng.,
Suez Canal University, Port-Said, Egypt

تحليل خصائص الاداء للمحرك التأثيري المفرد الوجه

الخلاصة: يقدم هذا البحث التحليل العددي للخصائص المغناطيسية والكهربية للمحرك التأثيري المفرد الوجه ذو المكثف المتجزيء - الدائم باستخدام طريقة العنصر المحدد الثنائي الابعاد أخذين في الاعتبار المجال الكهربي وجهد الاطراف. حسبت تيارات الملفات الرئيسية والمساعدة وتوزنت بالنتائج العملية ووجد الاتفاق بينهما جيد. تم حساب وتحليل وتوزيع الفيض وكثافة الفيض العظمى وكذلك توزيعات نسبة المحور والفقد الحديدي أخذين في الاعتبار التشبع المغناطيسي في القلب الحديدي وتأثير التيارات الإعصارية بموصلات العضو الدوار. وأخيرا تم تحليل ومناقشة منحنيات خصائص السرعة والخصائص السعوية للمحرك التأثيري المفرد الوجه ذو المكثف.

Abstract: This paper presents the numerical analysis of magnetic and electric characteristics of a permanent-split capacitor single-phase induction motor by the 2-dimensional finite element method which takes account the electric field and the terminal voltage. The main and auxiliary winding currents are calculated and compared with the measured values, good agreement is obtained. More precisely, the flux and maximum flux density distributions, axis-ratio and iron loss distributions are determined and analyzed taking into account the core saturation and secondary eddy current effect. The speed and capacitive characteristic curves of the capacitive motor are also analyzed and investigated.

1.INTRODUCTION

Induction motors are electromagnetically complex devices composed of an intricate and intimate arrangement of materials, which have a diversity of nonlinear and anisotropic physical properties, and which are in relative motion. To improve the efficiency of the induction motor, it is necessary to make good use of its material characteristic for design. It is known that the causes of the increase in iron loss are partial turbulence of flux, occurrence of rotating flux, stress and strain caused in the core. Therefore, it is important to secure the material characteristics of the core and to know the loss distribution in the apparatus by analysis for decrease of these losses. A method of calculating the effects of such material changes on motor performance is needed.

In 1970 the finite element method was applied by Silvester and Chari[1] to the analysis of electrical machinery. Since then, this method has been applied extensively to a.c and d.c generators[2,3], to transformers[4,5], and to induction motors[6-13]. Induction motor performance is customarily specified in terms of operation at constant excitation, and as a function of rotor speed. The electrical quantities which must therefore be determined as part of a performance analysis are the exciting currents. This paper will show how finite element electromagnetic analysis packages, PE2D[14], can be used in the calculation of single phase induction motor performance. The magnetic and electric performance characteristics of permanent-split capacitor motors are studied by using the 2-dimensional finite element method which takes into account the electric field and terminal voltage

2. THEORETICAL DEVELOPMENT

2.1 Preliminary Consideration And Assumptions

One of the features that makes the finite element method attrative for induction motor analysis is its ability to model nonlinear material properties. It is important that this capability be incorporated in the proposed method of analysis, so that iron saturation is included. A complete representation of the magnetic behaviour of the iron in a machine would require a time-stepping solution, with incremental changes in rotor position and the magnetic history of each individual iron element being stored. Although such an approach is possible, it is not as yet feasible, because the storage and processing time required would be prodigious. A number of simplifying assumptions are therefore made:

(a) Magnetic vector potential and current density have only the Z-axis component.
(b) Conductivity of laminated core is zero, and eddy current is ignored without the secondary conductor.
(c) The leakage flux is neglected in the air, and magnetic vector potential on the surface of the iron core is constant.
(d) The phase of the field changes 180 degrees per one pole, and slot ripple is ignored.
(e) Flux density varies sinuscidally with time at all points inside the machine.

2.2 Formulation of The Field Equations

The standard approach to solving electromagnetic field problems by the finite element method is to express Maxwell's equations in terms of the magnetic vector potential as follows;

$$\nabla \times E = -\partial B/\partial t = -j\omega B$$

$$\nabla \times H = J \qquad (1)$$

$$\nabla . B = 0$$

where displacement currents are neglected. E, B, H, and J are the electric field intensity, magnetic flux density, magnetic field intensity and current density respectively. The vector potential A is defind by

$$\nabla \times A = B \qquad (2)$$

The magnetisation characteristic representing the relationship between the magnetic field vectors is generally given as:

$$H = \nu B \qquad (3)$$

where ν is the reluctivity of the medium and a function of magnetic induction B . Equations(1)-(3) can be combined and written explicity as

$$\nu[\nabla \times (\nabla \times A)] = \sigma[E + v \times (\nabla \times A)] - J$$

$$= j s \omega \sigma A - J \qquad (4)$$

where s is slip, ω is the angular frequency of stator current, σ is conductivity and v is the velocity.
Equation(4) is reformulated by Galerkin weighted residual procedure, and first-order triangular elements are used to discretize the field region. Applying the Galerkin procedure over each element in turn yields a set of

linear simultaneous equations, which is solved using a preconditioned conjugate gradient method. The resulting magnetic vector potential are used to determine the performance characteristics of the motor.

2.3 Formulation of Circuit Equations

In general, the electric machinery and apparatus are excited by connecting the external constant power source. Then it is necessary that the characteristics are calculated under the constant terminal voltage.
The permanent-split capacitor motor of analytical model consists of two kinds of current circuits. The current circuit equations are calculated in the main and the auxiliary windings, that is, by Kirchhoff's second law.
First, in the main winding,

$$(d/dt)\int A.dS + (R_{cm} + R_m)I_m + L_m(dI_m/dt) = V \qquad (5)$$

Then in the auxiliary winding,

$$(d/dt)\int A.dS + (R_{ca} + R_a)I_a + L_a(dI_a/dt) + (1/C)\int I_a.dt = V \qquad (6)$$

where R_m and R_a are the resistances of the main and auxiliary windings respectivily. R_{cm} and R_{ca} are the external resistances. L_m and L_a are the leakage inductances. I_m and I_a are the currents flowing in each conductor. V is the terminal voltage. C is the capacitance.

3. RESULTS AND DISCUSSION

3.1 Analytical Model

The algorithm described in section 2 was developed for use in the study of a particular type of induction motor. Fig.(1) shows the structure and dimension of analyzed single-phase squirrel-cage induction motor. This motor has 4-pole, and the rated voltage, frequency and power are 100 V, 50 Hz and 0.1 Kw, respectively. Gap length 0.5 mm. It is driven by connecting the 14 μf capacitor in the auxiliary winding. Fig.(2) shows the subdivision of finite element region by first order triangular element. Numbers of elements and nodes are 1122 and 608 respectively.

3.2 Main And Auxiliary Winding Currents

By finite element method which takes into account the terminal voltage, unknown current values are obtained with the magnetic vector potential of each node. The computational currents flowing in the main and auxiliary windings are compared with the measured values, at 100 V and 50 Hz, as

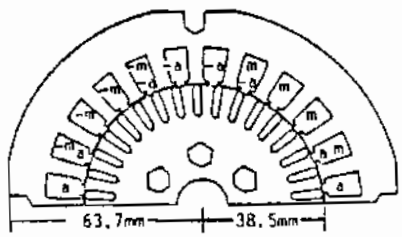

Fig.(1) Analytical model
m :main winding m.c:⊙
a :auxiliary winding a.c:⊗

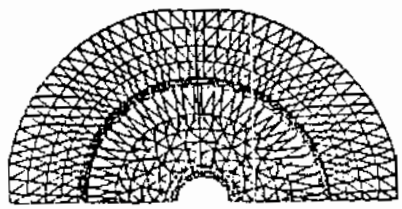

Fig.(2) Finite element meshes

shown in fig.(3). In this figure, black points are the measured values and white are the calculated ones. Both values are in good agreement with each other. Above all, the finite element method which takes into account the terminal voltage is a reasonably good method for analyzing the motor which consists of two or more current circuits whether steady or not.

3.3 Flux and Maximum Flux Density Distributions

The magnetic flux distributions at (a) slip s=1 and (b) slip s=0.03 are shown in fig.(4). Where standard time is the moment when supplied voltage is zero. When slip is small, the eddy current in the secondary conductor is small. Therefore, the flux passes through the inside of rotor because of small effect of the field caused by eddy current. But when slip is large, the eddy current shows a large value. Then the flux from stator makes the fluctuation of the whole rotor. Above this, the results show that flux distribution is asymmetrical in each pole. These results point out that electric field can not be ignored.

Hysterisis loss gives a large effect to the maximun flux density. Fig.(5) shows the distribution of maximum flux density at (a) s=1 and (b) s=0.03 . In this figure, equi-maximum flux density line is drawn by step 0.2 tesla. When slip is large, the value of flux density is small as compared with the

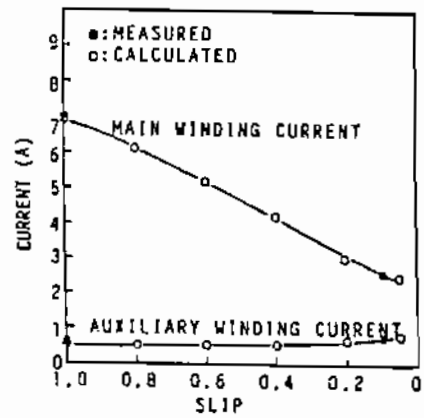

Fig.(3)Comparison between measured values and computational results of exciting current.

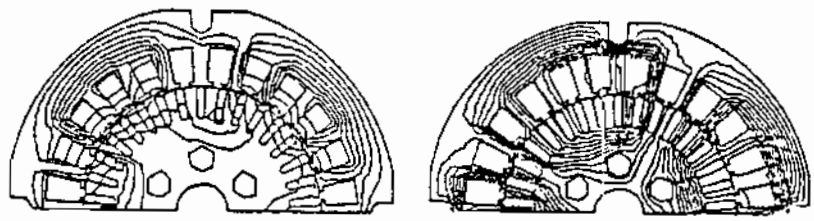

(a)s=1 (b)s=0.03

Fig.(4)Flux distributions

case of small slip. In the teeth and the behind part, the flux density shows large value in both conditions. The values of the maximum flux density are very different in each part. This is the cause which makes the vibration and the noise in the single phase induction motor, and which reduces its efficiency.

3.4 Axis-Ratio and Iron Loss Distributions

The axis-ratio is the ratio between maximum and minimum flux density. Axis ratio 1 and 0 mean the circular flux and alternating flux respectively. Fig.(6) shows the axis-ratio distribution at (a) s=1 and (b) s=0.03 . The rotating flux with large axis-ratio appears partially in the stator yoke. Its values show that the iron loss caused by rotating flux is large partially. The partial iron loss is computed by equation(7)[8]. Here the applied upper limit of flux density is 1.4 tesla.

$$W = K\,B_{max}^{1.95} + (1.319/B_{max} + 1.198)\,B_{min}^{1.69} \qquad W/Kg \qquad (7)$$

$$\begin{aligned} 0 \leq B_{min} &< 0.75 \quad K = 2.62 \\ 0.75 \leq B_{min} &< 1.25 \quad K = 2.30 \\ 1.25 \leq B_{min} &< 1.75 \quad K = 2.71 \end{aligned}$$

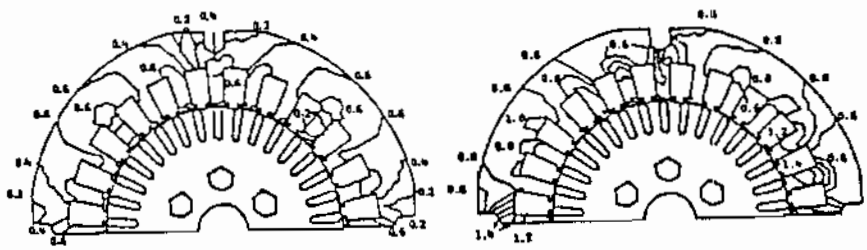

(a) s = 1 (b) s = 0.031

Fig.(5) Maximum flux density distributions

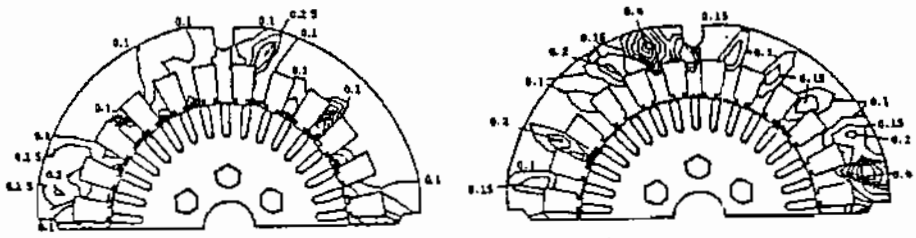

(a) s = 1 (b) s = 0.031

Fig.(6) Axis-ratio distributions

Fig.(7) shows the iron loss distribution, where the distribution is similar to the distribution of the maximum flux density. In this figure, the large iron loss is ordinarily caused in the part of large axis-ratio. But the large iron loss is seen in spite of the small axis-ratio. It is because the alternating flux iron loss is larger than the rotating flux iron loss. As a result, the turbulence of the flux increases the partial iron loss. That is in the groove part, it is necessary to discuss in the design for the shape of iron core.

3.5 Speed and Capacitive Characteristics

Figure (8) shows the speed characteristic curves. Where power factor is calculated by the current values obtained in fig.(3) and the efficiency is calculated by the iron loss obtained with eqn.(7). The mechanical loss is ignored. In this figure, the efficiency takes the maximum value when slip is nears 0.1 .

Since the permanent-split capacitor motor is ordinarily connected to a constant capacitance, the capacity of which is selected middle of the optimum value when its starting and exciting. Then, fig.(9) shows the capacitive characteristics at (a) s=1 and (b) s=0.03 respectively.

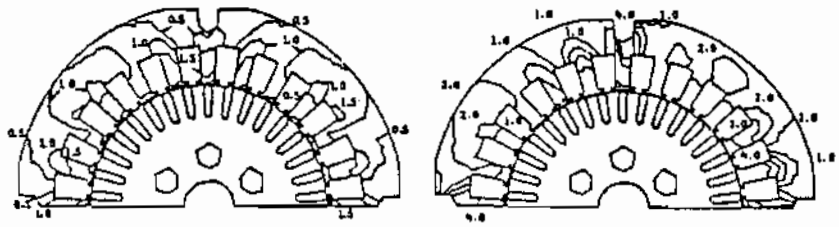

(a) s = 1 (b) s = 0,03

Fig.(7)Iron loss distributions

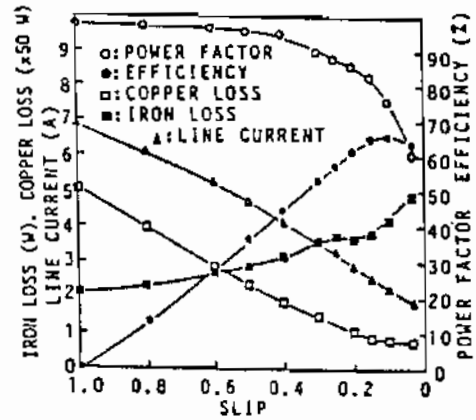

Fig.(8)Speed characteristic curves

4. CONCLUSIONS

This paper proposed a flexible and efficient technique for analyzing the magnetic and electric characteristics of a permanent-split capacitor single phase induction motor. The technique is based on the 2-dimensional finite element electromagnetic field analysis. Main conclusions drawn from this study are as follows:

(1)Due to low loss and high efficiency of the induction motor, it is necessary to secure the material characteristics used in it and to know the inner loss distribution of the motor with regard to its material.

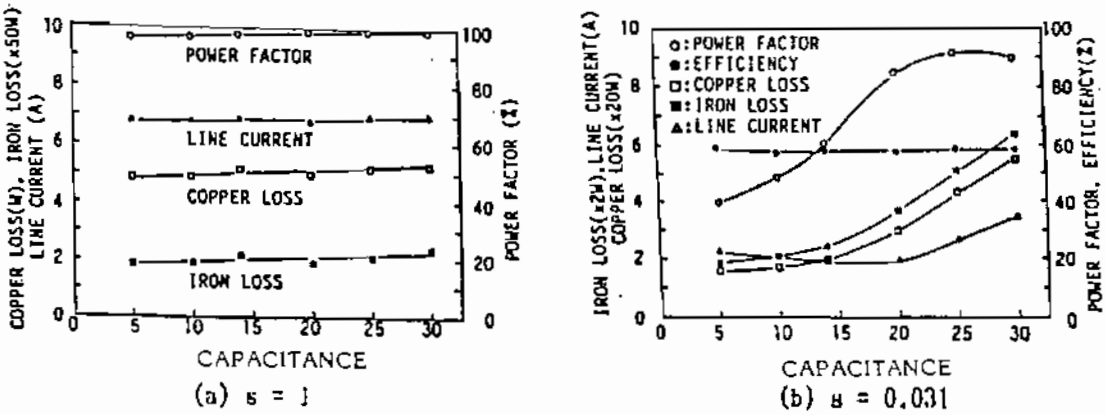

Fig.(9)Capacitive characteristics

(2)The eddy current flowing in the secondary conductor has a large effect to the flux distribution in the iron core. The effect varies by the slip value.

(3)The excellent agreement between numerical and experimental results verifies the numerical technique developed in this paper.

5. REFERENCES

1. Silvester, P.,and Chari,M.V.K.,"Finite element solution of saturable magnetic field problems", IEEE Trans., Vol.PAS-89, pp.1642-52, Sept 1970.
2. Chari, M.V.K.,and Silvester, P.,"Analysis of turbo-alternator magnetic fields by finite elements", IEEE Trans.,Vol.PAS-90,pp.454-64,March 1971.
3. Chari, M.V.K.,and Silvester, P.,"Finite element analysis of magnetically saturated D.C machines", IEEE Trans., Vol.PAS-90,pp.2362-72,Sept 1971.
4. Andersen, O.W.,"Transformer leakage flux program based on the finite element method", IEEE Trans., Vol.PAS-92,pp.682-9, March 1973.
5. Brauer, J.R.,"Finite element analysis of electromagnetic induction in transformers", paper A77-122-5, IEEE PES Winter Meeting, Feb 1977.
6. Ito,M., Okuda,H.,Takahashi,N.,and Miyata,T.,"Analytical model for magnetic field analysis of induction motor performance", IEEE Trans., Vol.PAS-100, pp.4582-90, 1981.
7. Silvester, P., Cabayon, H.S.,and Browne, B.T.,"Efficient techniques for finite element analysis of electrical machines", IEEE Trans., Vol.PAS-92 pp.1274-81, 1973.
8. Brauer, J.R.,"Finite element analysis of single phase and polyphase induction motors", paper B23-482-88, IEEE IAS, 1981.
9. Williamson, S.,and Ralph,J.W,"Finite element analysis of an induction motor fed from a constant-voltage source", IEE Proc., Vol.130, Pt-B, No.1, pp.18-24, 1983.
10. Amin, I.A. and El-Deeb,H.E,"Finite elemrnt analysis of 2-D field in the air gap and slot of electrical machines", Engineering Research Bulletin, Univ. of Helwan, Vol.6,pp.48-59, 1988.
11. Amin, I.A.,"The finite element contribution to electrical machine design Manscura Engineering Journal, Vol.14, No.1, pp.1-9, 1989.
12. Amin, I.A.,"Analysis of magnetic forces in induction motors due to non uniform air gap", Ain Shams Scient. Bulletin,Vol.24,No.2,pp.124-35,1989.
13. Amin, I.A.,"Finite element analysis of noise from small single phase induction machines", Engineering Research Bulletin, University of Helwan Vol.7, pp.274-87, Dec 1991.
14. Biddlecombe, C., Riley, C.,and Simkin, J.,"PE2D user guide", Rutherford Appleton Laboratory, Oct 1983.